Journal of Catalysis 279 (2011) 174–182

Contents lists available at ScienceDirect

Journal of Catalysis

journal homepage: www.elsevier.com/locate/jcat

Design of solid acid catalysts for aqueous-phase dehydration of carbohydrates: The role of Lewis and Brønsted acid sites

Ronen Weingarten, Geoffrey A. Tompsett, Wm Curtis Conner Jr., George W. Huber *

Department of Chemical Engineering, University of Massachusetts Amherst, 159 Goessmann Lab, 686 North Pleasant St., Amherst, MA 01003-9303, United States

ARTICLE INFO

Article history:
Received 4 November 2010
Revised 13 January 2011
Accepted 15 January 2011
Available online 24 February 2011

Keywords:
Acid catalyst
Dehydration
Xylose
Furfural
Brønsted
Lewis

ABSTRACT

We have prepared a series of well-characterized acid catalysts, including Zr–P, SiO_2–Al_2O_3, WO_X/ZrO_2, γ-Al_2O_3, and HY zeolite and tested them for aqueous-phase dehydration of xylose. We have characterized the concentration of both Brønsted and Lewis acid sites in these catalysts with TPD and FT-IR spectroscopy using gas-phase NH_3 and compared the catalytic activity and selectivity with that of homogeneous catalysts for the dehydration of aqueous solutions of xylose. The catalyst selectivity is a function of the Brønsted to Lewis acid site ratio for both the heterogeneous and homogeneous reactions. Lewis acid sites decrease furfural selectivity by catalyzing a side reaction between xylose and furfural to form humins (insoluble degradation products). At 20% xylose conversion, catalysts with high Brønsted to Lewis acid ratios, such as Zr–P, exhibit furfural selectivities as much as 30 times higher than catalysts with higher Lewis acid site concentrations. Dehydration reactions using ion-exchange polymer resins with high Brønsted acid site concentrations showed similar selectivities to Zr–P and HCl. Using HY zeolite revealed a low furfural selectivity due to strong irreversible adsorption of the furfural in the pores, causing an increase in the rate of humin formation. Thus, to design more efficient aqueous-phase dehydration catalysts, it is desirable to have a high ratio of Brønsted to Lewis acid sites. Furthermore, gas-phase characterization of acid sites can be used to predict catalytic activity in the aqueous phase.

1. Introduction

Biomass is a renewable feedstock that can be used for fuels and chemicals production. The transformation of biomass to fuels primarily calls for the decrease in the effective oxygen to carbon molar ratio. Dehydration is one of the key reactions that can be used to remove oxygen from the biomass feedstocks [1]. Dehydration of carbohydrates leads to the formation of furan compounds such as furfural and HMF, which can serve as intermediates for production of liquid alkanes and other furan-based chemicals [2–8]. Dehydration reactions have also been shown to play vital roles in liquid-phase catalytic processing and aqueous-phase reforming to produce jet and diesel fuel range alkanes from biomass-derived oxygenated hydrocarbons [9–12].

Furfural is a product of the triple dehydration reaction of xylose. Furfural can be used as a feedstock to make both gasoline, diesel, or jet fuel [13,14]. We have recently developed an intrinsic kinetic model for the dehydration of xylose in a biphasic reaction scheme using a homogeneous catalyst (HCl) [15]. Fig. 1 depicts the overall reaction scheme. Xylose first undergoes a triple dehydration reaction to form furfural (Reaction 1). Furfural and xylose can then react together to form undesired solid humins, which are highly polymerized insoluble carbonaceous species (Reaction 2). Furfural can also react with itself to form solid humins (Reaction 3). In a biphasic regime, the furfural can be extracted into an organic solvent (Reaction 4), and this step is governed by mass transfer. Reactions 1–3 are all first order with respect to their reactants. Reaction 2 is the dominant reaction to form humins. The activation energy for the dehydration reaction is higher (E_A = 124 kJ mol^{-1}) than the activation energy for humin formation from Reaction 2 (E_A = 72 kJ mol^{-1}) or Reaction 3 (E_A = 68 kJ mol^{-1}).

At present, furfural is produced commercially using batch or continuous reactors with a mineral acid (i.e., sulfuric acid) [16]. Many studies have reported on the dehydration of xylose to form furfural with homogeneous acid catalysts [3,6,17,18]. Even though promising results have been attained, it would be desirable to obtain solid catalysts that exhibit activities and selectivities at least comparable to homogeneous catalysts for aqueous-phase dehydration. Solid catalysts are advantageous due to their economic and environmental viability. Industrially, they are preferred due to the ease of postreaction catalyst separation. Valente and co-workers have reported various studies on the design of solid acid catalysts for the dehydration of xylose to produce furfural. Their work spans over a broad range of catalytic materials including modified mesoporous silicas [19–22], exfoliated transition metal oxides [23],

* Corresponding author. Fax: +1 413 545 1647.
E-mail addresses: rweingarten@ecs.umass.edu (R. Weingarten), tompsett@ecs.umass.edu (G.A. Tompsett), wconner@ecs.umass.edu (Wm. C. Conner Jr.), huber@ecs.umass.edu (G.W. Huber).

0021-9517/$ - see front matter © 2011 Elsevier Inc. All rights reserved.
doi:10.1016/j.jcat.2011.01.013

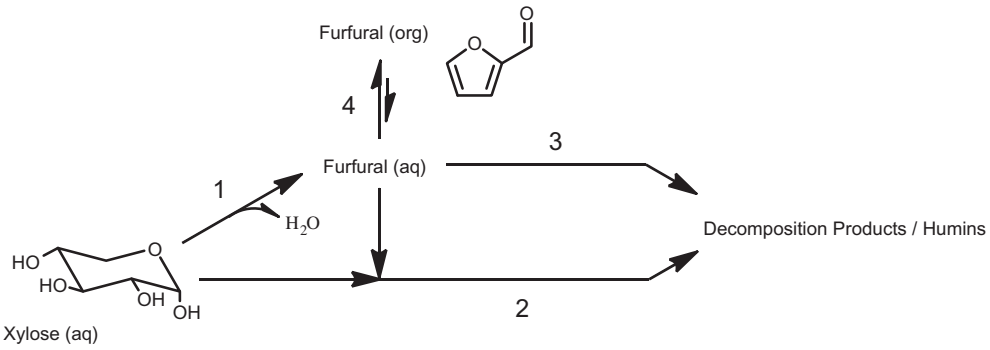

Fig. 1. Xylose dehydration reaction scheme.

sulfated metal oxides [24], and microporous silicoaluminophosphates [25].

Large-scale furfural production consists of treating agricultural waste materials rich in pentosan polymers with sulfuric acid. This resulting mixture is then treated with steam where the steam extracts the furfural from the solid biomass producing a dilute aqueous stream containing water and furfural [16]. The ability to efficiently execute the dehydration step with solid catalysts in a biphasic regime could be beneficial from both an economical and ecological point of view. With that being said, there are still many unanswered questions pertaining to the behavior of solid catalysts in aqueous solutions. An area of particular focus is the interfacial interactions between aqueous solutions and metal oxides. The metal oxide–water interface is reactive due to a range of chemistries, including acid–base, ligand exchange, and/or redox [26]. In general, the exposure of solid oxides to water gives rise to electrical charges on the solid surface. This is due to hydration effects that can involve H^+ and OH^- ions from the bulk aqueous phase. Incomplete coordination of the exposed metal or oxide ions at the solid surface is the cause of this phenomenon [27]. As a result, positive and negative sites are present on the solid surface, and the excess of one type of site determines the net charge. For aqueous solutions, this is a function of the pH. The solution pH at which the net charge on the surface is zero is known as the point of zero charge (PZC). The surface has a net positive charge when the solution pH is below the PZC, and a net negative charge when the solution pH is above the PZC [28]. Comprehensive studies on the PZC of various metal oxides and hydroxides have been reported by Parks and Kosmulski [29–34].

Contrary to biomass conversion, solid catalysts in the oil and petrochemical industries are typically used in gas phase or in liquid phase, where the reaction medium is usually non-polar.[1] Well-established techniques have been developed to characterize acid–base surface properties in the gas phase, such as adsorption–desorption, calorimetry, and IR spectroscopy [35]. On the catalyst surface, Brønsted acid sites (proton donors) can be generated from highly polarized hydroxyl groups. They can also form on oxide-based catalysts *via* proton balance of a net negative charge introduced by substituting cations with a lower valence charge [36]. Alternatively, Lewis acid sites form from coordinatively unsaturated cationic sites, which leave M^{n+} exposed to interact with guest molecules as an acceptor of an electron pair [1]. Exposure of the catalyst to a polar solvent such as water can potentially alter the intrinsic nature of the acid surface due to solvation effects. For instance, the hydroxyl ion from the water molecule (Lewis base) can react with a Lewis site (M^{n+}) on the surface to generate Brønsted sites [35,37–39]. Others have reported that the primary effect of water is displacement of strongly adsorbed basic probe molecules from the acid sites [40,41]. Poisoning of the acid sites by water may also occur depending on the surface hydrophilicity/hydrophobicity of the catalyst [42]. Even so, the existence of Lewis acid sites in aqueous media has been recognized. Davis and co-workers have shown that tin-containing zeolites are highly active catalysts for the isomerization of glucose in water [43]. The mechanism consists of an intramolecular hydride shift catalyzed by tin which behaves as a Lewis acid in water [44].

This reality in turn poses difficulties in determining the acidity of solid acids in aqueous media. One approach is to determine the number of Brønsted sites in water from the number of free protons arising from cation exchange with a salt in aqueous solution at the surface of the solid [45–49]. Aqueous-phase titration is a common method used for quantification purposes. The concentration of acid sites can also be estimated by *poisoning* of the active sites with a base and measuring the catalytic activity versus poison concentration [35]. Shanks and co-workers have found that the conditions under which aqueous-phase titrations are performed have to be chosen carefully as they can have a significant effect on the measured values [50]. Other techniques for acid site characterization have been reviewed by Tanabe [51].

The objective of this study is to examine the role of Lewis and Brønsted sites of solid acid catalysts for the dehydration of carbohydrates in aqueous media. Dehydration of xylose to produce furfural was chosen as the model reaction. Our results will allow us to deduce the optimal design of solid acid catalysts for this class of reactions. We compare two common methods of characterizing the acid content of the catalysts, including titration in the liquid phase and temperature-programmed desorption in the gas phase.

2. Experimental

2.1. Catalyst preparation

The zirconium phosphate catalyst (Zr–P) was prepared following procedures previously reported in the literature [52], which consisted of precipitation of $ZrCl_2O{\cdot}8H_2O$ (Sigma Aldrich, 1 mol L^{-1}, 70 mL) and $NH_4H_2PO_4$ (Sigma Aldrich, 1 mol L^{-1}, 140 mL) at a molar ratio of P/Zr = 2. The solution was stirred and then filtered, washed with de-ionized (DI) water and dried overnight at 373 K. The catalyst was calcined at 673 K for 4 h in air prior to reaction. This Zr–P was confirmed to be amorphous by XRD. The SiO_2–Al_2O_3 catalyst (Sigma Aldrich grade 135, Si/Al = 5.0) was calcined at 773 K for 16 h in air. HY catalyst (Zeolyst CBV 720, Si/Al = 30) was calcined at 813 K for 16 h in air. Tungstated zirconia catalyst (WO_X/ZrO_2, XZO 1251) with WO_3 content 15 wt.% was supplied by MEL Chemicals. This catalyst was calcined in air at 873 K for 4 h to remove water and organic contaminants. The γ-Al_2O_3 catalyst was obtained by calcining alumina boehmite CATAPAL B supplied by Sasol at 873 K for 4 h in air. The crystal structure was confirmed by XRD. The Nafion SAC-13 (Sigma Aldrich) and Amberlyst 70 (Rohm and Haas) were dried overnight at 383 K

and crushed. The latter was sieved to a particle size of ⩽125 μm. Hydrochloric acid was supplied by Fisher Scientific. Ytterbium (III) trifluoromethanesulfonate hydrate, $Yb(OTf)_3$, was supplied by Strem Chemicals. The Brønsted and Lewis acid sites for each solid catalyst are portrayed in Table 1.

2.2. Catalyst characterization

Total acid sites were determined by ammonia temperature-programmed desorption (NH_3-TPD) [60] with a Quantachrome ChemBET Pulsar™ TPR/TPD Automatic Chemisorption Analyzer coupled with a Thermal Conductivity Detector (TCD) to quantify the ammonia desorbed from the sample. A sample of 300 mg was initially degassed at 773 K for 1 h under a constant helium flow of 60 mL min^{-1} (Airgas, UHP). The sample was cooled, and ammonia (Airgas, electronic grade) was adsorbed at 373 K. After saturation, the ammonia supply line was shut off, and helium was purged at 60 mL min^{-1} to remove any physically adsorbed ammonia. The sample was then heated linearly at a rate of 10 K min^{-1} from 373 to 873 K (973 K for Zr–P) under a constant helium flow of 60 mL min^{-1}. The sample was held at the temperature set point for an additional 1 h.

The Brønsted to Lewis acid site ratio of the catalysts was determined by FT-IR spectroscopy with ammonia as a probe molecule [61,62]. The spectra were recorded on a Bruker Equinox 55 spectrometer at a resolution of 4 cm^{-1} (averaging 50 scans). A Harrick Scientific "Praying Mantis" Diffuse Reflectance Infrared cell (DRIFTS) allowed for in situ recording of the spectra at ambient temperature and catalyst activation at higher temperatures. The cell was equipped with a heater and connected to a gas flow system. The temperature was monitored with a thermocouple placed in direct contact with the sample. Powder samples (~20 mg) were loaded into the DRIFTS cell for FT-IR spectroscopy studies. A spectrum of KBr (taken at ambient temperature before) was used as a background reference. Before the surface characterization was performed, the samples were activated by heating at 673 K for 2 h under helium (Airgas, UHP) flow of 20 mL min^{-1}, cooled down to 373 K, and saturated with ammonia (Airgas, anhydrous 99.99%) for 20–30 min. The gas flow was then switched back to helium (20 mL min^{-1}) to remove physically adsorbed ammonia, and the spectrum monitored until no change was observed (~30 min). The samples were then heated in helium flow (20 mL min^{-1}) to various temperatures. The spectra were recorded at each temperature up to 873 K. All of the spectra were obtained by subtraction of the corresponding background reference spectra. Data analysis and peak fitting were carried out using GRAMS/AI® software (Thermo-Scientific). The ion-exchange polymer resins were analyzed by FT-IR spectroscopy according to a previously reported method with pyridine as a probe molecule [63].

The BET surface areas and pore volumes were determined by nitrogen adsorption at 77 K using a Quantachrome Autosorb®-1-C automated gas sorption system. The samples were evacuated before each experiment at 523 K for 24 h (423 K for ion-exchange resins). As the BET method overestimates the surface area of microporous material, an empirical estimation technique was used. This consisted of subtracting the adsorbed volume of adsorbate in the

Table 1
Illustration of the Brønsted and Lewis acid sites for each solid catalyst.

Catalyst[a]	Brønsted sites	Lewis sites
Zr–P [53,54]	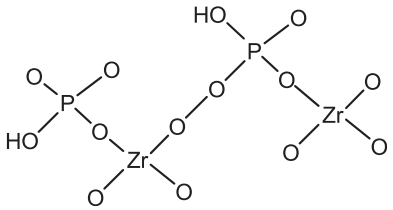	
SiO_2–Al_2O_3 [35,42]	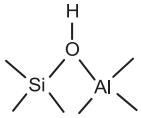	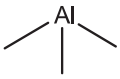
HY		
WO_x/ZrO_2 [55–57]	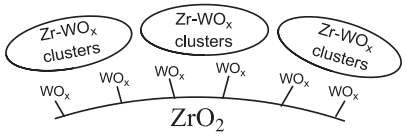	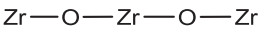
γ-Al_2O_3 [37]	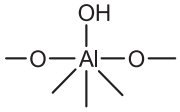	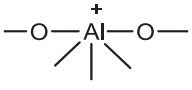
Nafion SAC-13 [58]	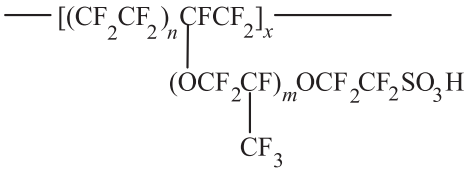	N/A
Amberlyst 70 [59]	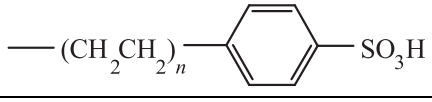	N/A

[a] References to figures.

microporous region (typically $P/P_o < 10^{-4}$) from the remaining adsorption points and recalculating the surface area by using the BET method and obtaining the appropriate "C" constant.

Liquid adsorption experiments with aqueous solutions of xylose and furfural were performed in accordance with the literature [41]. A known amount of catalyst (0.15 g) was mixed with 10 g of a 2 wt.% solution of DI water and the adsorbate. The mixture was stirred for 19–22 h at room temperature to ensure that equilibrium was reached, followed by filtration with a 0.2-μm syringe filter to remove the catalyst. Desorption studies were carried out by separating the catalyst from the liquid phase with a centrifuge following the adsorption procedure. DI water was then added to the retained catalyst, and the mixture was stirred for additional 22 h at room temperature to ensure that equilibrium was reached. The mixture was finally filtered with a 0.2-μm syringe filter to remove the catalyst. The amounts of adsorbate/desorbate present in the liquid phase were determined with the analysis method stated below.

The catalytic acid sites in the aqueous phase were determined by a titration method previously reported in the literature [64]. A sodium hydroxide aqueous solution (0.01 mol L^{-1}, 20 mL) was mixed with a known amount of catalyst for 2 h at room temperature. The solution was then filtered with a 0.2-μm syringe filter and titrated by a hydrochloric acid solution (0.1 mol L^{-1}). The equivalence point (EQP) was detected by using a Mettler-Toledo© T50 auto-titrator. Phenolphthalein indicator was used as well for qualitative purposes.

2.3. Catalyst activity

Reactions were carried out in the Discover™ System (CEM Corporation) with an 80-mL batch reactor. Xylose dehydration reactions consisted of an aqueous solution of 10 wt.% xylose (Acros Organics) unless otherwise stated. Furfural decomposition reactions consisted of 1.5 wt.% furfural (Acros Organics) unless otherwise stated. All of the aqueous solutions were prepared with DI water. Throughout all of the experiments, the total number of acid sites was held constant at 0.500 mmoles (determined by NH_3-TPD) unless otherwise stated, and the amount of loaded reaction solution was kept constant at 30 g. All solutions were mixed at a maximum constant rate using a magnetic stir bar. Temperatures in the reactor were measured by way of a fiber optic sensor. The reaction vessel was pressurized due to the vapor pressure of the solution at the defined reaction temperature. A dip tube was inserted into the reaction media for sampling purposes. Samples were immediately quenched with ice and filtered with a 0.2-μm syringe filter prior to analysis.

2.4. Analysis

Samples were analyzed by liquid chromatography with a Shimadzu© LC-20AT. Xylose was detected with a RI detector (RID-10A), and products were detected with a UV–Vis detector (SPD-20AV) at wavelengths of 210 and 254 nm. The column used was a Biorad© Aminex HPX-87H sugar column. The mobile phase was 0.005 M H_2SO_4 flowing at a rate of 0.6 mL/min. The column oven was set to 30 °C. Total organic carbon (TOC) measurements were performed with a Shimadzu© TOC-VCPH Analyzer. Calibrations were performed with carbon standards supplied by SpectroPure.

3. Results

3.1. Characterization of solid acid catalysts

The solid acid catalysts were characterized both in the gaseous and aqueous phase. The characterization data appear in Table 2 in descending order of Brønsted to Lewis acid site ratio. Adsorption experiments were performed with both xylose and furfural as adsorbates at room temperature in the aqueous phase. Xylose did not adsorb on any of the catalysts at room temperature. Furfural adsorption uptakes were found to be similar for all of the catalysts with the exception of HY which had an uptake of up to seven times the amount of the other catalysts on a per gram basis. This result is higher than that reported by Tsapatsis and co-workers for furfural adsorption on faujasite zeolite (Si/Al = 30) [41]. Additional desorption experiments with HY showed that only 27% of the adsorbed furfural on the catalyst desorbed back into the aqueous phase.

The number of acid sites calculated from the aqueous-phase titration was different than those calculated by ammonia-TPD. The aqueous-phase method showed an increased number of acid sites compared to the number of acid sites obtained with the gaseous sorption technique. This could be due to the adsorption of sodium hydroxide (titrant) on inactive sites as well as on the active acid sites of the catalysts throughout the titration process [35]. Even so, the concentration of acid sites measured by aqueous-phase titration increased with the ratio of Brønsted to Lewis acid sites determined by ammonia FT-IR spectroscopy in the gas phase.

The acid concentrations obtained from the aqueous (titration) and gaseous techniques (NH_3-TPD) were not comparable to each other. With the exception of γ-Al_2O_3, the results obtained from aqueous-phase titration are higher than those from the gas-phase sorption technique. Several studies have been reported on titration techniques, with some stating that aqueous-phase titration solely quantifies Brønsted sites [51,64]. To validate these claims, we carried out additional titration experiments at constant Brønsted sites (according to NH_3-TPD). Similarly, we also performed titrations while keeping the total number of acid sites constant (according to NH_3-TPD). Arbitrary and inconsistent results on both attempts raise doubts about the validity of this aqueous-phase characterization technique (refer to Table S1). Similar conclusions have been previously reported [38,39,51].

3.2. Xylose dehydration and furfural degradation

Xylose dehydration was studied with the different solid acid catalysts in the aqueous phase at 160 °C with the total acid sites held constant at 0.500 mmoles (according to NH_3-TPD). Fig. 2

Table 2
Characterization of solid acid catalysts.

Catalyst	Gas-phase characterization					Aqueous-phase characterization	Furfural adsorption
	BET surface area ($m^2\ g^{-1}$)	Micropore volume ($cm^3\ g^{-1}$)	Brønsted:Lewis ratio	Total acid sites (mmol g^{-1})	Brønsted sites (mmol g^{-1})	Acid sites (mmol g^{-1})	Uptake ($g\ g^{-1}$)
Zr–P	168	0	27.00	1.413	1.362	4.250	0.07
SiO_2–Al_2O_3	585	0	3.78	0.432	0.342	1.450	0.06
HY	303[a]	0.028	1.50	0.520	0.312	1.047	0.30
WO_X/ZrO_2	149	0	0.74	0.324	0.138	0.875	0.05
γ-Al_2O_3	262	0	0.67	0.428	0.171	0.124	0.04

[a] Estimated using microporous subtraction method. BET "C" constant is 68.

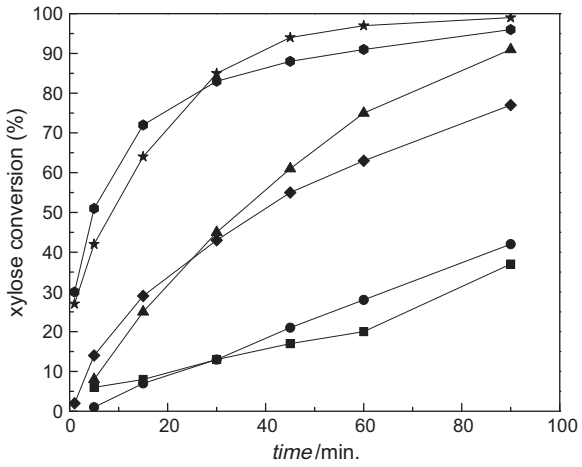

Fig. 2. Aqueous-phase xylose dehydration at 160 °C with different solid acid catalysts. Total acid sites were kept constant at 0.500 mmoles (determined by NH_3-TPD). Feed was 10 wt.% xylose aqueous solution. Catalysts: HCl (■), Zr–P (●), SiO_2–Al_2O_3 (▲), HY (♦), WO_X/ZrO_2 (⬢), and γ-Al_2O_3 (★).

depicts xylose conversion as a function of reaction time for the various catalysts. The catalytic activity was found not to be a function of the total number of acid sites as measured by NH_3-TPD. However, the catalysts with the highest number of Lewis acid sites were found to be the most active. On a per site basis, the catalytic activity decreased as follows: γ-Al_2O_3 ~ WO_X/ZrO_2 > SiO_2–Al_2O_3 ~ HY > Zr–P ~ HCl. Increasing the relative number of Brønsted to Lewis acid sites decreased the catalytic activity.

The furfural selectivity as a function of conversion is shown in Fig. 3. The furfural selectivity decreased as follows: Zr–P ~ HCl ≫ SiO_2–Al_2O_3 > WO_X/ZrO_2 > HY > γ-Al_2O_3. This follows the opposite trend compared to catalyst activity. Thus, the catalysts that are most active demonstrate the lowest selectivity for furfural production. The Zr–P and HCl catalysts have significantly higher furfural selectivities than the other four catalysts. The furfural selectivity increases with xylose conversion for the other four catalysts. These experiments show that the furfural selectivity is dependent on the type of acid catalyst site.

Additional stability studies with Zr–P, SiO_2–Al_2O_3, and WO_X/ZrO_2 have shown that the catalysts retain their total acid concentrations after exposure to water at 160 °C (refer to Table S2). This was confirmed by NH_3-TPD following filtration and recalcination of the catalysts. Further testing was performed on Zr–P that consisted of mixing Zr–P in DI water for 1.5 h at 160 °C, followed by hot filtration to separate the catalyst. Xylose was then added to the filtrate to produce an aqueous solution of 10 wt.% xylose. We then proceeded to dehydrate the xylose in a blank experiment (no additional catalyst). A comparable blank study was also carried out for an aqueous solution of 10 wt.% xylose consisting of clean DI water. Results from both experiments were practically identical, indicating that the acid sites on Zr–P do not leach in aqueous media. This agrees with conclusions made by Li et al. who found Zr–P to be stable in aqueous media at high temperatures (245 °C). They found that for aqueous-phase hydrodeoxygenation of sorbitol no deactivation occurred for Pt/Zr–P after 200 h time-on stream. ICP studies confirmed that no leaching occurred [65].

Furfural itself can undergo degradation reactions to form humins [15]. Separate experiments were performed with furfural as the feedstock (1.5 wt.%) to study the effect of the catalysts on furfural degradation as shown in Fig. 4. Reactions took place at 160 °C with total acid sites held constant at 0.500 mmoles (according to NH_3-TPD). In these experiments, furfural was converted into a water insoluble humin phase that could not be detected by HPLC analysis. The catalyst activity was determined by measuring the residual amount of furfural in the aqueous phase. TOC measurements were performed to predict the overall carbon balance, and results showed that we can account for all of the carbon. Formic acid was also detected as a minor by-product of this reaction. Williams and Dunlop suggested that the presence of formic acid is a result of hydrolytic fission of the furfural aldehyde group [66,67].

Furfural degradation (disappearance) was found to be fairly independent of the catalyst used, with the exception of HY which had a significantly higher rate of furfural disappearance. This concurs with the HY adsorption/desorption data which showed a relatively high uptake of furfural. Further reactions with furfural as the feedstock and HY at various mixing rates confirmed that the reaction with this catalyst was not limited by external mass transfer. HY behaves differently from the other catalysts as it has a microporous structure (see Table 2). This suggests that microporous materials of this nature are undesirable for aqueous-phase dehydration reactions of xylose because they demonstrate higher rates of furfural disappearance. These experiments show that the furfural degradation is a function of the amount of acid sites on

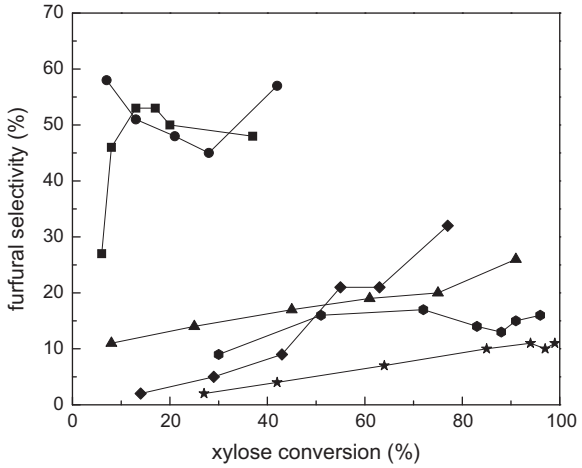

Fig. 3. Furfural selectivity as a function of xylose conversion for different solid acid catalysts at 160 °C. Total acid sites were kept constant at 0.500 mmoles (determined by NH_3-TPD). Feed was 10 wt.% xylose aqueous solution. Catalysts: HCl (■), Zr–P (●), SiO_2–Al_2O_3 (▲), HY (♦), WO_X/ZrO_2 (⬢), and γ-Al_2O_3 (★).

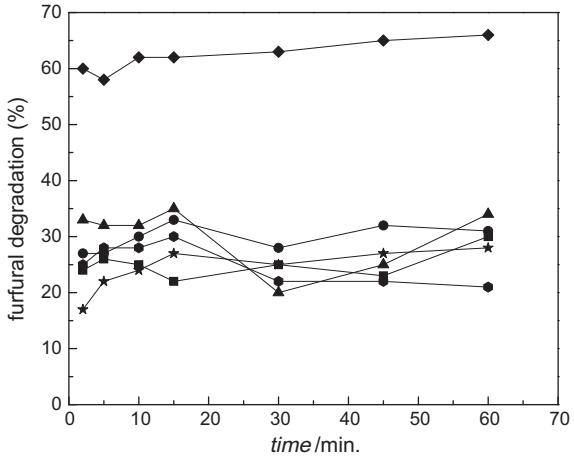

Fig. 4. Furfural degradation (disappearance) with different acid catalysts at 160 °C. Total acid sites were kept constant at 0.500 mmoles (determined by NH_3-TPD). Feed was 1.5 wt.% furfural aqueous solution. Catalysts: HCl (■), Zr–P (●), SiO_2–Al_2O_3 (▲), HY (♦), WO_X/ZrO_2 (⬢), and γ-Al_2O_3 (★).

the catalyst surface. Humins can also form from reactions between xylose and furfural, which we have previously shown to be the dominant pathway for humin formation for the aqueous-phase dehydration of xylose with HCl [15].

3.3. Dehydration reactions with homogeneous Brønsted and Lewis acids

Water-soluble Brønsted and Lewis acids were used for xylose dehydration reactions in the aqueous phase. Hydrochloric acid and ytterbium (III) trifluoromethanesulfonate hydrate, $Yb(OTf)_3$, were used, respectively. The latter is considered a stable water-soluble Lewis acid [42,68]. Reactions were performed at varying Brønsted to Lewis ratios by combining the two acids accordingly, while holding the total amount of acid constant at 0.500 mmoles. Fig. 5 shows the conversion of xylose for the different ratios of catalysts. The pure $Yb(OTf)_3$ catalyst had the highest activity for xylose disappearance, while the pure HCl showed the lowest activity. A mixture of $Yb(OTf)_3$ and HCl had a moderate catalyst activity. This result indicates that the Lewis acid sites have a higher catalytic activity toward xylose disappearance compared to the Brønsted acid sites, which is consistent with the results from the heterogeneous catalysts.

The furfural selectivity as a function of conversion is shown in Fig. 6. HCl has a significantly higher furfural selectivity compared to $Yb(OTf)_3$. This signifies that the nature of the acid site can significantly affect the furfural selectivity, with Brønsted acid sites being more selective toward furfural production than Lewis acid sites. Again, these results are consistent with those of the heterogeneous catalysts.

Additional studies were performed at lower temperatures using a feedstock comprised of a mixture of xylose and furfural. Reactions were carried out with HCl and $Yb(OTf)_3$ separately. A 1:1 M ratio of xylose and furfural was used with the total number of acid sites held constant at 0.750 mmoles. The results appear in Table 3.

The results obtained with HCl coincide with the reaction scheme in Fig. 1. Reaction 1 (xylose dehydration) did not occur at the low reaction temperature due to its relatively high activation energy compared to Reactions 2 and 3. The latter reactions were suppressed as a result of the negligible amounts of furfural present. This is confirmed by the negligible xylose conversion and furfural yield. A similar outcome was attained with a feedstock composed of xylose and furfural.

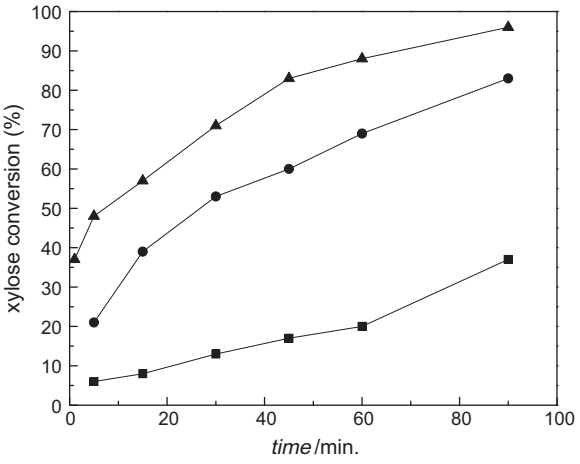

Fig. 5. Effect of Brønsted to Lewis acid ratio on xylose conversion in a homogeneous regime at 160 °C. Total acid sites were kept constant at 0.500 mmoles. Feed was 10 wt.% xylose aqueous solution. Brønsted: Lewis ratio = 1:0 (■), 1:1 (●), and 0:1 (▲).

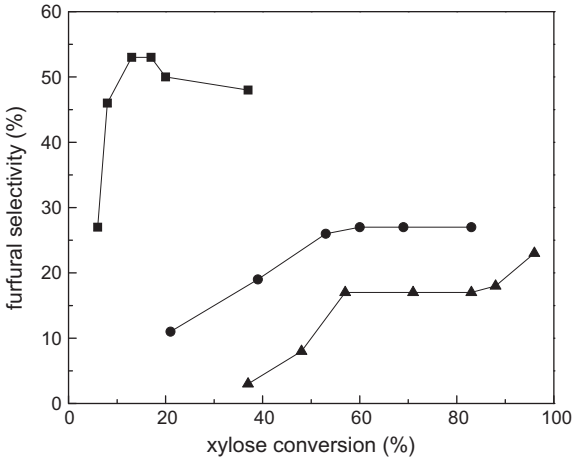

Fig. 6. Effect of Brønsted to Lewis acid ratio on furfural selectivity from xylose in a homogeneous regime at 160 °C. Total acid sites were kept constant at 0.500 mmoles. Feed was 10 wt.% xylose aqueous solution. Brønsted:Lewis ratio = 1:0 (■), 1:1 (●), and 0:1 (▲).

Table 3
Results from dehydration reactions with homogeneous acid catalysts at 88 °C. Feeds were 3 wt.% xylose, 2 wt.% furfural, or a mixture of the both (1:1 M ratio). Total acid sites were kept constant at 0.750 mmoles. Reaction time was 90 min.

Catalyst	Feedstock	Xylose conversion (%)	Furfural conversion (%)	Furfural yield (%)	Humins yield (%)
HCl	Xylose	5.7	–	0.4	5.3
	Furfural	–	11.4	–	10.4
	Xylose + furfural	4.9	6.6	–	5.3
$Yb(OTf)_3$	Xylose	28.5	–	0.5	27.5
	Furfural	–	7.4	–	7.4
	Xylose + furfural	27.1	13.9	–	17.4

Reactions with the homogeneous Lewis acid catalyst $Yb(OTf)_3$ resulted in relatively high xylose conversions and humins yields. The low reaction temperature and negligible furfural yield reduce the likelihood that this was due to xylose dehydration to produce furfural (Reaction 1). Rather, this was due to a new reaction pathway with xylose reacting with itself to produce humins.

3.4. Furfural production with ion resin catalysts

Xylose dehydration reactions were performed with acidic ion-exchange polymer resins to show the significance of Brønsted acid sites on furfural selectivity. Resins such as Nafion and Amberlyst have been shown to be effective catalysts for a wide range of acid-catalyzed reactions [58,69]. Dumesic and co-workers used Nafion SAC-13 and Amberlyst 70 in part to produce liquid hydrocarbon transportation fuels. The catalysts were found to be particularly active for the dehydration of 5-nonanol to form nonenes with subsequent oligomerization to form C_9-derived alkenes [70]. This is primarily due to their relatively high concentrations of Brønsted acid sites. The characterization data for the ion resins appear in Table 4.

Xylose conversion was measured as a function of time for Nafion SAC-13, Amberlyst 70, Zr–P, and HCl as shown in Fig. 7. The catalytic activity of Zr–P was found to be the highest compared to the ion resins and HCl. This coincides with our previous results that found catalyst activity to increase with the concentration of Lewis acid sites. The ion resins and HCl contain only Brønsted acid sites, whereas Zr–P contains Lewis sites as well. Nafion SAC-13 showed lower xylose conversions than Amberlyst 70 and HCl. We believe

Table 4
Characterization of acidic ion-exchange polymer resins.

Catalyst	Gas-phase characterization					Aqueous-phase characterization	Furfural adsorption
	BET surface area ($m^2\ g^{-1}$)	Micropore volume ($cm^3\ g^{-1}$)	Brønsted: Lewis ratio	Total acid sites (mmol g^{-1})	Brønsted sites (mmol g^{-1})	Acid sites (mmol g^{-1})	Uptake ($g\ g^{-1}$)
Nafion SAC-13	231	0	∞[b]	0.140[a]	0.140	0.881	0.10
Amberlyst 70	0.32	0	∞	2.860[a]	2.860	3.176	0.13

[a] Data provided by manufacturer.
[b] FT-IR analysis detected weak Lewis acid sites originating from the silica matrix [60]. These sites were inactive in xylose dehydration.

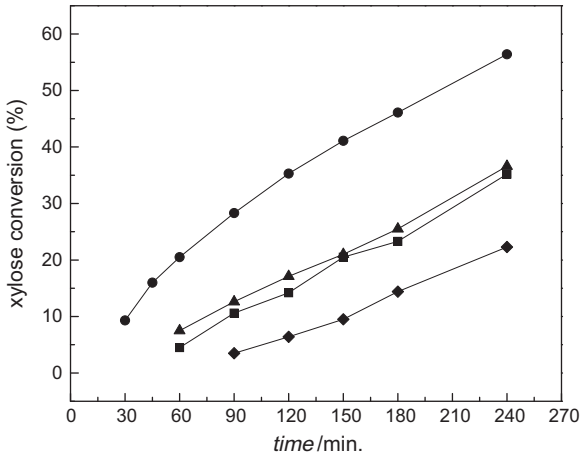

Fig. 7. Xylose conversion as a function of time for different solid acid catalysts at 160 °C. Total acid sites were kept constant at 0.150 mmoles (data determined by NH_3-TPD or taken from manufacturer). Feed was 3 wt.% xylose aqueous solution. Catalysts: HCl (■), Zr–P (●), Amberlyst 70 (▲), and Nafion SAC-13 (♦).

that this is due to mass transfer limitations in the reactor due to inadequate mixing of the catalyst.

Fig. 8 compares the furfural selectivities as a function of xylose conversion for Nafion SAC-13, Amberlyst 70, Zr–P, and HCl. The results were found to be comparable for all of the catalysts.

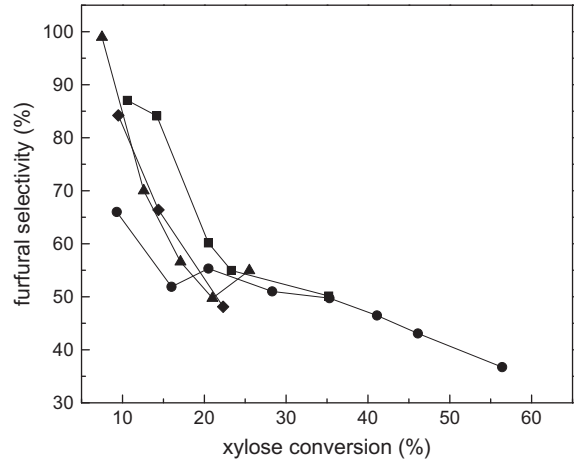

Fig. 8. Furfural selectivity as a function of xylose conversion for different solid acid catalysts at 160 °C. Total acid sites were kept constant at 0.150 mmoles (data determined by NH_3-TPD or taken from manufacturer). Feed was 3 wt.% xylose aqueous solution. Catalysts: HCl (■), Zr–P (●), Amberlyst 70 (▲), and Nafion SAC-13 (♦).

4. Discussion

The reaction chemistry for furfural production is comprised of three key reactions and a phase equilibrium relationship (applicable in a biphasic system). Xylose undergoes dehydration to lose three water molecules and produce furfural (Reaction 1); xylose reacts with furfural to produce humins (Reaction 2), and furfural undergoes a mono-degradation reaction to produce humins (Reaction 3). We have demonstrated here that Lewis and Brønsted sites share different functions as related to our proposed reaction scheme for xylose dehydration. Our studies show that both types of acid sites catalyze the dehydration of xylose to produce furfural (Reaction 1). Similarly, furfural decomposes on both Brønsted and Lewis sites to form humins (Reaction 3). Reaction 2, on the other hand, is predominantly catalyzed by Lewis sites. Consequently, a higher rate of xylose disappearance and lower furfural selectivity are observed for catalysts with increased Lewis sites. We have also showed that Lewis sites catalyze xylose mono-decomposition at lower temperatures. This reaction pathway could potentially be significant at higher temperatures as well.

Similar conclusions have been deduced by Song-Hai et al. in their study of acrolein production by gas-phase dehydration of glycerol with solid acid catalysts [71]. They found Brønsted acid sites to be advantageous over Lewis acid sites in selectively producing acrolein. They did not attempt to explain the cause of the undesired degradation reactions leading to lower acrolein selectivity. Likewise, in their study of furfural formation by acid hydrolysis of rice-hulls, Islam et al. found the addition of metal chlorides (Lewis acids) to have a negative effect on the furfural yield [72]. In regard to furfural, it has been suggested that the formation of black resinous products, i.e., humins, is a result of the furfural furan ring as well as the aldehyde group participating in polymerization reactions [73]. Accordingly, given the favorable conditions, Lewis acids can form stable adducts with furfural, which can possibly lead to the further formation of highly complex structures.

Initial reaction rates were deduced from the experimental plots of concentrations versus time using OriginPro® 7.5 software. The relative reaction rates for humin formation by furfural degradation (Reaction 3) and humin formation by reaction of furfural with xylose (Reaction 2) are shown in Table 5. For this purpose, humins were considered all non-detectable soluble and insoluble compounds. These reaction rates are reported in reference to Reaction 1, which is furfural production. The relative rate of Reaction 2 increases with the concentration of Lewis acid sites. The relative rate of Reaction 3 is similar for all catalysts except for the HY and WO_X/ZrO_2. The high relative rate of Reaction 3 observed for HY, as depicted in Table 5, confirms that induced degradation reactions occur due to the irreversible adsorption of furfural in the catalyst pores. This concurs with previous conclusions made by Lourvanij et al. in their studies of glucose dehydration to oxygenated hydrocarbons with microporous materials [74–76]. They claim that microporous catalysts such as HY zeolite induce molecular sieving reactions within the pores to

Table 5
Relative reaction rates calculated in accordance with xylose dehydration scheme.

Catalyst	Fraction of Brønsted acid sites	Relative rates	
		$Rate_2/Rate_1$	$Rate_3/Rate_1$
HCl	1.00	7.52	39.02
Zr–P	0.96	3.73	46.94
SiO_2–Al_2O_3	0.79	20.42	54.12
HY	0.60	54.05	140.56
WO_X/ZrO_2	0.43	25.26	5.71
γ-Al_2O_3	0.40	167.93	20.84

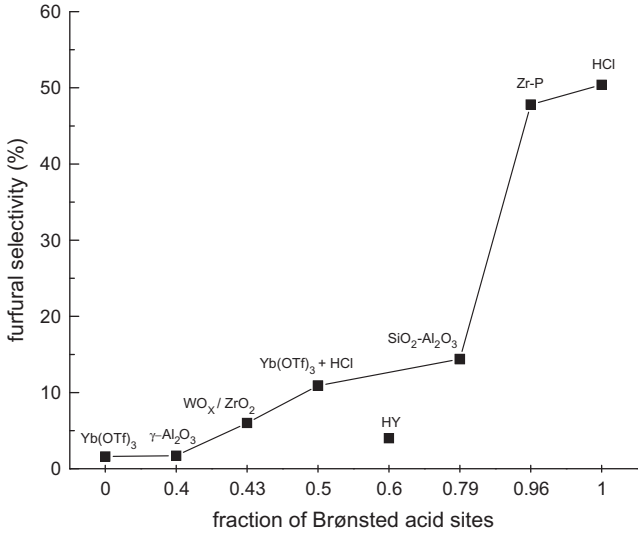

Fig. 9. Furfural selectivity as a function of the fraction of Brønsted acid sites at 20% xylose conversion and 160 °C. Total acid sites were kept constant at 0.500 mmoles. Feed was 10 wt.% xylose aqueous solution.

promote the formation of coke. In comparison, they showed that a considerable less amount of decomposition reactions occurred with mesoporous MCM catalysts.

Fig. 9 shows the furfural selectivity as a function of the fraction of Brønsted acid sites for the heterogeneous and homogeneous catalysts tested in this paper. These results clearly show that the furfural selectivity is a function of the Brønsted to Lewis acid site ratio as measured by the gas-phase characterization. Thus, solid acid catalysts with high Brønsted to Lewis acid site ratios are necessary in order to obtain high furfural selectivities. A low concentration of Lewis acid sites minimizes the undesirable formation of humins *via* Reaction 2. Furthermore, dehydration reactions with acidic ion-exchange polymer resins show comparable furfural selectivities with Zr–P and HCl. Similarly, Dias et al. showed that furfural can be produced from xylose at high selectivities (70%) and conversions (90%) with Amberlyst 15 [19]. These results confirm that furfural selectivity is a direct function of the Brønsted acid sites concentration and not necessarily the nature of the acid sites.

It is notable to mention that all reactions in this paper were carried out by way of microwave heating. We performed some preliminary experiments on xylose dehydration to compare microwave heating with conventional heating with a heterogeneous catalyst. When HCl was used as a catalyst, no difference in the rate of xylose conversion or furfural selectivity was observed with microwave and conventional heating [15]. However, when Zr–P was used as a catalyst, the rate of xylose conversion with microwave heating was between 1.92 and 3.32 times that of conventional heating depending on reaction time (refer to Fig. S1). Conventional reactions took place in a Parr reactor, and identical heating rates were employed for all reactions in this comparison. The furfural selectivity was slightly higher for microwave heating than conventional heating with the Zr–P catalyst (refer to Fig. S2). Our current findings agree with those reported by Qi et al. who showed enhanced production of 5-hydroxymethylfurfural (HMF) from fructose and glucose due to microwave irradiation [77,78]. Accordingly, it has been emphasized that microwave absorption at the solid interface can advantageously influence the overall reaction kinetics [79]. Further studies are necessary to fully understand the enhanced microwave effects reported for systems with heterogeneous catalysts.

5. Conclusions

We have prepared a series of well-characterized acid catalysts and tested them for aqueous-phase dehydration of xylose to furfural. We have determined the concentration of both Brønsted and Lewis acid sites of these catalysts with gas-phase techniques and compared the results with those obtained with a titration technique in the aqueous phase. For four out of the five catalysts tested, the titration studies resulted in higher acid concentrations compared to the gas-phase technique. These inconsistent results raise questions about the reliability of the aqueous-phase characterization techniques. Furthermore, the consistent data that we have obtained from dehydration reactions in aqueous solutions with the solid acid catalysts confirm that gas-phase characterization of acid sites can be used to predict catalytic activity in the aqueous phase.

The catalytic activity of the various solid acid catalysts for xylose dehydration in the aqueous phase is not a function of the total number of acid sites as measured by NH_3 adsorption or NaOH titration. On a per site basis, γ-Al_2O_3 shows the highest activity, whereas Zr–P and HCl demonstrate the lowest. Furfural selectivity follows the opposite trend with Zr–P and HCl having considerably higher furfural selectivities than the other four catalysts. This finding confirms that furfural selectivity is dependent on the type of acid catalyst site.

The function of Lewis and Brønsted acid sites has been established in reference to the kinetic model that we developed for xylose dehydration. Lewis and Brønsted sites are responsible for catalyzing the dehydration reaction of xylose to form furfural (Reaction 1), as well as the degradation of furfural to form humins (Reaction 3). Lewis sites are principally accountable for the decrease in furfural selectivity due to the reaction between xylose and furfural to form humins (Reaction 2). Lewis sites can also potentially decrease the furfural selectivity by catalyzing the mono-decomposition of xylose to form humic compounds.

Furfural selectivity increases with an increase in the Brønsted to Lewis acid site ratio of the catalyst. This has been confirmed with both heterogeneous and homogeneous acids. Catalysts with high Brønsted to Lewis acid site ratios, such as Zr–P, show selectivities as much as 30 times higher than catalysts with increased Lewis acid sites at 20% xylose conversion. These results are comparable with those obtained from dehydration reactions with acidic ion-exchange polymer resins and HCl. Additionally, Zr–P shows viable promise for dehydration reactions due to its catalytic stability in the aqueous phase at high temperatures.

Catalyst pore confinement has an adverse effect on furfural selectivity. Adsorption–desorption studies in the aqueous phase and decomposition experiments with furfural in aqueous solutions have confirmed that HY zeolite causes furfural to irreversibly adsorb in the zeolite pores and polymerize to form humic substances. Therefore, it can be concluded that microporous catalysts of this nature are undesirable for xylose dehydration reactions due to strong adsorption of the product in the catalyst pore which leads to undesirable decomposition reactions.

Acknowledgments

The authors gratefully acknowledge financial support from NSF-CBET (Grant # 0756663) and NSF MRI (Grant # 0722802). We also sincerely thank Ieva Narkeviciute for providing the FT-IR spectroscopic data. Dr. Wenqin Shen is acknowledged for her technical assistance and thoughtful discussions and Christopher Kalinowski for his contribution in the laboratory.

Appendix A. Supplementary data

Supplementary data associated with this article can be found, in the online version, at doi:10.1016/j.jcat.2011.01.013.

References

[1] R. Rinaldi, F. Schuth, Energy and Environmental Science 2 (2009) 610–626.
[2] C. Moreau, M.N. Belgacem, A. Gandini, Topics in Catalysis 27 (2004) 11–30.
[3] Y. Roman-Leshkov, J.N. Chheda, J.A. Dumesic, Science 312 (2006) 1933–1937.
[4] J.N. Chheda, J.A. Dumesic, Catalysis Today 123 (2007) 59–70.
[5] Y. Roman-Leshkov, C.J. Barrett, Z.Y. Liu, J.A. Dumesic, Nature 447 (2007) 982–985.
[6] J.N. Chheda, Y. Roman-Leshkov, J.A. Dumesic, Green Chemistry 9 (2007) 342–350.
[7] R. West, Z. Liu, M. Peter, J. Dumesic, ChemSusChem 1 (2008) 417–424.
[8] Y. Roman-Leshkov, J.A. Dumesic, Topics in Catalysis 52 (2009) 297–303.
[9] G.W. Huber, R.D. Cortright, J.A. Dumesic, Angewandte Chemie International Edition 43 (2004) 1549–1551.
[10] G.W. Huber, S. Iborra, A. Corma, Chemical Reviews 106 (2006) 4044–4098.
[11] R.R. Davda, J.W. Shabaker, G.W. Huber, R.D. Cortright, J.A. Dumesic, Applied Catalysis B: Environmental 56 (2005) 171–186.
[12] R. Xing, A.V. Subrahmanyam, H. Olcay, W. Qi, G.P. van Walsum, H. Pendse, G.W. Huber, Green Chemistry 12 (2010) 1933–1946.
[13] S. Bayan, E. Beati, La Chimica e L'Industria 23 (1941) 432–434.
[14] G.W. Huber, J.N. Chheda, C.J. Barrett, J.A. Dumesic, Science 308 (2005) 1446–1450.
[15] R. Weingarten, J. Cho, W.C. Conner, G.W. Huber, Green Chemistry 12 (2010) 1423–1429.
[16] R.H. Kottke, 2000. Furan derivatives. In: Kirk-Othmer Encyclopedia of Chemical Technology. John Wiley & Sons, pp. 259–286.
[17] B. Sain, A. Chaudhuri, J.N. Borgohain, B.P. Baruah, J.L. Ghose, Journal of Scientific and Industrial Research 41 (1982) 431–438.
[18] A.S. Dias, M. Pillinger, A.A. Valente, Applied Catalysis A: General 285 (2005) 126–131.
[19] A.S. Dias, M. Pillinger, A.A. Valente, Journal of Catalysis 229 (2005) 414–423.
[20] A.S. Dias, M. Pillinger, A.A. Valente, Microporous and Mesoporous Materials 94 (2006) 214–225.
[21] A. Dias, S. Lima, P. Brandão, M. Pillinger, J. Rocha, A. Valente, Catalysis Letters 108 (2006) 179–186.
[22] S. Lima, M.M. Antunes, A. Fernandes, M. Pillinger, M.F. Ribeiro, A.A. Valente, Molecules 15 (2010) 3863–3877.
[23] A.S. Dias, S. Lima, D. Carriazo, V. Rives, M. Pillinger, A.A. Valente, Journal of Catalysis 244 (2006) 230–237.
[24] A. Dias, S. Lima, M. Pillinger, A. Valente, Catalysis Letters 114 (2007) 151–160.
[25] S. Lima, A. Fernandes, M. Antunes, M. Pillinger, F. Ribeiro, A. Valente, Catalysis Letters 135 (2010) 41–47.
[26] G.E. Brown, V.E. Henrich, W.H. Casey, D.L. Clark, C. Eggleston, A. Felmy, D.W. Goodman, M. Gratzel, G. Maciel, M.I. McCarthy, K.H. Nealson, D.A. Sverjensky, M.F. Toney, J.M. Zachara, Chemical Reviews 99 (1998) 77–174.
[27] R.O. James, Advances in Ceramics 21 (1987) 349–410.
[28] G.V. Franks, Y. Gan, Journal of the American Ceramic Society 90 (2007) 3373–3388.
[29] G.A. Parks, Chemical Reviews 65 (1965) 177–198.
[30] M. Kosmulski, Journal of Colloid and Interface Science 253 (2002) 77–87.
[31] M. Kosmulski, Journal of Colloid and Interface Science 275 (2004) 214–224.
[32] M. Kosmulski, Journal of Colloid and Interface Science 298 (2006) 730–741.
[33] M. Kosmulski, Journal of Colloid and Interface Science 337 (2009) 439–448.
[34] M. Kosmulski, Advances in Colloid and Interface Science 152 (2009) 14–25.
[35] T.S. Glazneva, N.S. Kotsarenko, E.A. Paukshtis, Kinetics and Catalysis 49 (2008) 859–867.
[36] D.G. Barton, M. Shtein, R.D. Wilson, S.L. Soled, E. Iglesia, The Journal of Physical Chemistry B 103 (1999) 630–640.
[37] B. Kasprzyk-Hordern, Advances in Colloid and Interface Science 110 (2004) 19–48.
[38] L. Forni, Catalysis Reviews 8 (1973) 65–115.
[39] H.A. Benesi, B.H.C. Winquist, Advances in Catalysis, Academic Press, Inc., New York, pp. 97–182.
[40] A.P. Kulkarni, D.S. Muggli, Applied Catalysis A: General 302 (2006) 274–282.
[41] R. Ranjan, S. Thust, C.E. Gounaris, M. Woo, C.A. Floudas, M.v. Keitz, K.J. Valentas, J. Wei, M. Tsapatsis, Microporous and Mesoporous Materials 122 (2009) 143–148.
[42] T. Okuhara, Chemical Reviews 102 (2002) 3641–3666.
[43] M. Moliner, Y. Roman-Leshkov, M.E. Davis, Proceedings of the National Academy of Sciences 107 (2010) 6164–6168.
[44] Y. Roman-Leshkov, M. Moliner, J.A. Labinger, M.E. Davis, Angewandte Chemie International Edition 49 (2010) 8954–8957.
[45] A. Grenall, Industrial and Engineering Chemistry 41 (1949) 1485–1489.
[46] C.J. Plank, Analytical Chemistry 24 (1952) 1304–1306.
[47] V.C.F. Holm, G.C. Bailey, A. Clark, Journal of Physical Chemistry 63 (1959) 129–133.
[48] Y. Matsumura, S. Hagiwara, H. Takahashi, Carbon 14 (1976) 163–167.
[49] S. Neffe, Carbon 25 (1987) 441–443.
[50] B. Cinlar, Acid Catalyzed Carbohydrate Degradation and Dehydration in Chemical and Biological Engineering, Iowa State University, Ames, 2010.
[51] K. Tanabe, Solid Acids and Bases: Their Catalytic Properties, Kodansha Scientific Books, Tokyo, 1970.
[52] Y. Kamiya, S. Sakata, Y. Yoshinaga, R. Ohnishi, T. Okuhara, Catalysis Letters 94 (2004) 45–47.
[53] K.N. Rao, A. Sridhar, A.F. Lee, S.J. Tavener, N.A. Young, K. Wilson, Green Chemistry 8 (2006) 790–797.
[54] S.N. Pavlova, V.A. Sadykov, G.V. Zabolotnaya, D.I. Kochubey, R.I. Maximovskaya, V.I. Zaikovskii, V.V. Kriventsov, S.V. Tsybulya, E.B. Burgina, A.M. Volodin, M.V. Chaikina, N.N. Kuznetsova, V.V. Lunin, D. Agrawal, R. Roy, Journal of Molecular Catalysis A: Chemical 158 (2000) 319–323.
[55] E.I. Ross-Medgaarden, W.V. Knowles, T. Kim, M.S. Wong, W. Zhou, C.J. Kiely, I.E. Wachs, Journal of Catalysis 256 (2008) 108–125.
[56] W. Zhou, E.I. Ross-Medgaarden, W.V. Knowles, M.S. Wong, I.E. Wachs, C.J. Kiely, Nature Chemistry 1 (2009) 722–728.
[57] K. Shimizu, T.N. Venkatraman, W. Song, Applied Catalysis A: General 224 (2002) 77–87.
[58] M.A. Harmer, W.E. Farneth, Q. Sun, Journal of the American Chemical Society 118 (1996) 7708–7715.
[59] A. Molnar, Current Organic Chemistry 12 (2008) 159–181.
[60] G.L. Woolery, G.H. Kuehl, H.C. Timken, A.W. Chester, J.C. Vartuli, Zeolites 19 (1997) 288–296.
[61] E. Brunner, Catalysis Today 38 (1997) 361–376.
[62] J.N. Kondo, R. Nishitani, E. Yoda, T. Yokoi, T. Tatsumi, K. Domen, Physical Chemistry Chemical Physics 12 (2010) 11576–11586.
[63] B. Török, I. Kiricsi, Á. Molnár, G.A. Olah, Journal of Catalysis 193 (2000) 132–138.
[64] A. Onda, T. Ochi, K. Yanagisawa, Green Chemistry 10 (2008) 1033–1037.
[65] N. Li, G.A. Tompsett, G.W. Huber, ChemSusChem, vol. 3, pp. 1154–1157.
[66] D.L. Williams, A.P. Dunlop, Industrial and Engineering Chemistry 40 (1948) 239–241.
[67] A.P. Dunlop, Industrial and Engineering Chemistry 40 (1948) 204–209.
[68] A. Corma, H. Garcia, Chemical Reviews 103 (2003) 4307–4365.
[69] P.F. Siril, H.E. Cross, D.R. Brown, Journal of Molecular Catalysis A: Chemical 279 (2008) 63–68.
[70] D.M. Alonso, J.Q. Bond, J.C. Serrano-Ruiz, J.A. Dumesic, Green Chemistry 12 (2010) 992–999.
[71] S.-H. Chai, H.-P. Wang, Y. Liang, B.-Q. Xu, Green Chemistry 9 (2007) 1130–1136.
[72] A.M. Islam, S.M. Saad, M.S. Aboul-Fetouh, M.A. Sakran, Holzforschung 27 (1973) 117–123.
[73] T. Kunitake, K. Yamaguchi, C. Aso, Die Makromolekulare Chemie 172 (1973) 85–96.
[74] K. Lourvanij, G.L. Rorrer, Industrial and Engineering Chemistry Research 32 (1993) 11–19.
[75] K. Lourvanij, G.L. Rorrer, Applied Catalysis A: General 109 (1994) 147–165.
[76] K. Lourvanij, G.L. Rorrer, Journal of Chemical Technology and Biotechnology 69 (1997) 35–44.
[77] X. Qi, M. Watanabe, T.M. Aida, R.L. Smith Jr., Green Chemistry 10 (2008) 799–805.
[78] X. Qi, M. Watanabe, T.M. Aida, R.L. Smith Jr., Catalysis Communications 9 (2008) 2244–2249.
[79] W.C. Conner, G.A. Tompsett, Journal of Physical Chemistry B 112 (2008) 2110–2118.